

X-ray QPOs in Black-Hole Binary Systems

R. Remillard¹, M. Muno¹, J. McClintock² & J. Orosz³

¹ Center for Space Research, M.I.T., 77 Massachusetts Ave., Cambridge, MA 02139

² Harvard-Smithsonian Center for Astrophysics, 60 Garden St., Cambridge, MA 02139

³ Astronomical Institute, Utrecht University, Postbus 80000, 3508 TA Utrecht, The Netherlands.

Abstract. We briefly review the properties and physical consequences of quasiperiodic oscillations (QPOs) seen on many occasions in the X-ray emission from black-hole binary systems. High frequency QPOs ($\nu > 40$ Hz) continue to be scrutinized as effects of general relativity, with new attention to the role of resonances in their formation. Low-frequency QPOs (0.05 to 30 Hz) exhibit complicated behavior, with occasions of high amplitude and particular correlations with some X-ray spectral parameters. QPO mechanisms are a requirement for any physical model seeking to explain either (1) the non-thermal X-ray spectrum that is commonly seen and is usually stronger than the accretion disk at times of highest luminosity, or (2) the hard X-ray spectrum evident when there is a steady type of radio jet.

1. Introduction

Most of the brightest celestial X-ray sources recorded in a given year are transient outbursts from black hole binaries in the Galaxy. The eruptions are understood as a consequence of a low rate of mass accretion from the companion star [1]. The material gradually fills the outer regions of an accretion disk surrounding the black hole. When the disk surface density reaches a critical value, matter spirals into the inner disk where it reaches X-ray emitting temperatures before falling into the black hole event horizon [2]. Such X-ray novae are the parent population for identifying black holes that are remnants of massive stars. The mass of the compact object (typically 5–15 M_{\odot}) is deduced from radial velocity studies of the companion star. In most cases such measurements are only possible when the system has returned to relative quiescence, and the companion can be seen against the glare of the hot gases in the disk. In establishing the nature of the compact object, the critical argument is whether the mass exceeds the upper limit ($\sim 3.0 M_{\odot}$) for the mass of a neutron star. There are now 17 “dynamical black hole” binaries in the Milky Way or LMC: 14 were first noticed as bright X-ray novae [3], while the other 3 cases are persistent X-ray sources with O/B type companions.

Observations with the *Rossi* X-ray Timing Explorer (RXTE) have pioneered efforts to further study black holes and their occasional relativistic jets via broadband X-ray observations during active states of accretion. The X-ray timing and spectral properties convey information about physical processes that occur near the black hole event horizon, and one of the primary research goals is to obtain constraints on the black hole mass and spin using predictions of general relativity (GR) in the strong-field regime. There is also the need to understand accretion

physics for each of the four distinct emission states that are displayed by so many accreting black holes systems. In this paper we describe recent advances in these topics, with particular attention to the diverse forms of quasiperiodic oscillations (QPOs) [4] that have been detected during the extensive monitoring programs for X-ray transients conducted with RXTE.

2. High Frequency Oscillations in Accreting Black Hole Systems

The topic of high-frequency QPOs (HFQPOs) in black hole binaries (40-450 Hz) has evolved substantially in the last year. Transient HFQPOs are detected with RXTE in 5 sources (4 dynamical black holes and 1 candidate). These subtle oscillations have rms amplitudes that are typically only $\sim 1\%$ of the mean count rate. The associated power spectra are shown in Fig. 1, and their properties are summarized in Table 1. Three of these sources exhibit pairs of HFQPOs: GRO J1655–40 (300, 450 Hz; [5]), XTE J1550–564 (184, 276 Hz; [6, 7]), and GRS 1915+105 (40, 67; [8]). Furthermore, in Section 3 below we report the detection of additional HFQPOs in GRS 1915+105 at 164 and 328 Hz.

The commensurate frequencies (3:2 ratio) in pairs of HFQPOs from GRO J1655–40 and XTE J1550–564 [9] may suggest a cause in some type of resonance phenomenon involving oscillations proscribed by general relativity, as originally proposed by Abramowicz & Kluzniak [10]. The observations cannot be interpreted as non-sinusoidal structures in the wave pattern, in the sense of harmonics in a Fourier series, because the individual detections (in a given energy band) appear as a single peak in the power spectrum, and their frequencies are recognized as 2ν or 3ν only when the ensemble of results is examined.

TABLE 1. Table 1: High Frequency QPOs in Black Hole Systems

Source Name	# RXTE Obs.	QPO Freq. Hz (\pm)	Coherence ($\nu/FWHM$)	Detections # (3σ)	Energy (keV)	Ampl. rms %
GRO J1655–40	81	300 (23)	4.4–11.6	7	2–30	0.5–1.0
		450 (20)	8.8–14.8	6	13–30	2.5–5.3
XTE J1550–564	364	184 (26)	2.6–9.1	10	2–30	0.6–1.7
		272 (20)	4.7–14.3	14	6–30	3.6–6.9
GRS 1915+105	448	67 (5)	3.2–22.0	29	2–30	0.4–1.8
		41 (1)	5–20	5	13–30	1.8–3.2
		164 (2)	5–7	2 sums[14]	13–30	2.0–2.2
		328 (4)	14–16	2 sums[14]	13–30	1.0–1.3
4U 1630–47	301	184 (5)	5–9	sum[30]	6–30	1.0–1.2
XTE J1859+226	135	193 (4)	3–5	sum[48]	6–30	1.7–2.0

The resonance hypothesis [10] has been discussed in terms of accretion blobs following perturbed orbits in the inner accretion disk. Unlike Newtonian gravity, GR predicts independent oscillation frequencies for each spatial coordinate for orbits around a rotating compact object, as seen from the rest frame of a distant observer. GR coordinate frequencies and their differences (i.e. beat frequencies) have been proposed to explain some of the X-ray QPOs from both neutron stars

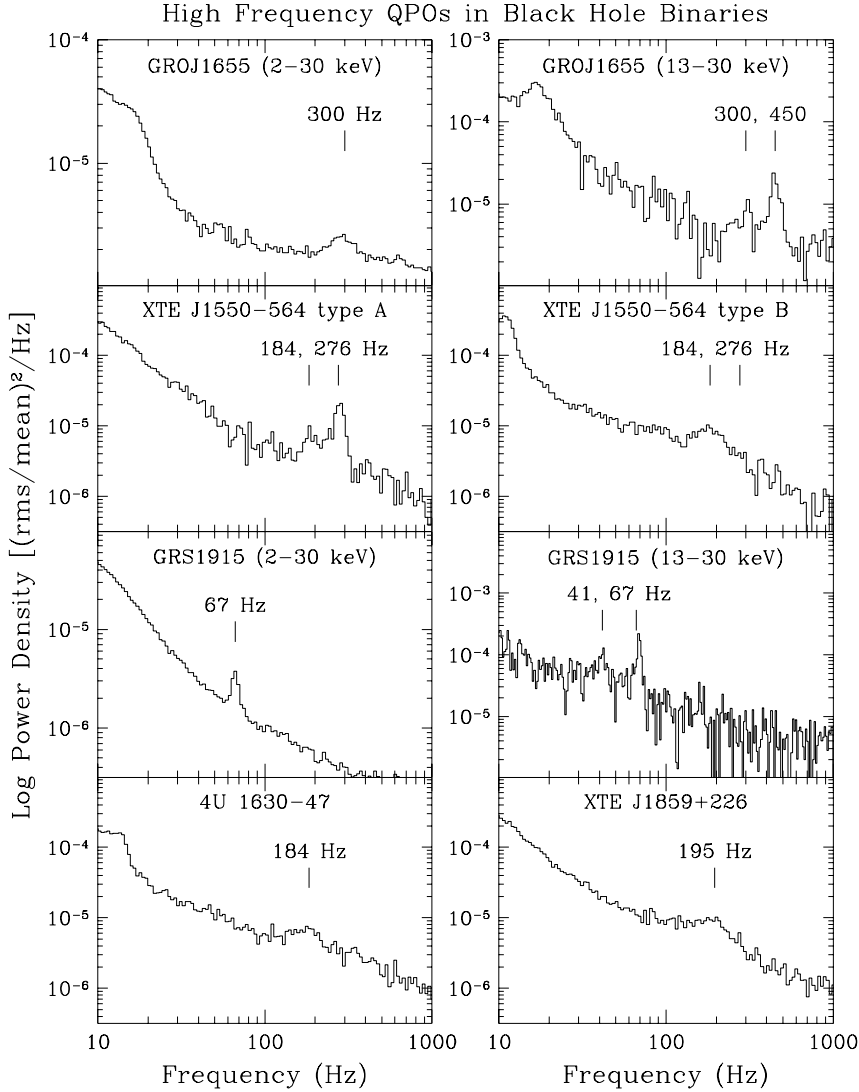


Figure 1. HFQPOs in five black hole binary systems. The energy band is 6-30 keV unless otherwise indicated. These subtle oscillations are only visible during a fraction of the observations for each source, and details are given in Table 1.

and black holes [11]. At the radii in the accretion disk where X-rays originate, the GR coordinate frequencies are predicted to have varying, non-integral ratios. The commensurate frequencies in pairs of HFQPOs, noted above, can therefore be interpreted as a signature of resonance, e.g. between pairs of coordinate frequencies in the inner disk. Unlike the azimuthal and polar coordinates frequencies, the radial coordinate frequency reaches a maximum value and then falls to zero as the radius decreases toward the location of the innermost stable orbit (see [12], [13], and references therein). This ensures the possibility of commensurate coordinate frequencies somewhere in the inner disk. For example, there is a wide range in

the dimensionless spin parameter, a_* , where one can find a particular radius that corresponds to a 2:1, 3:1, or 3:2 ratio in the orbital and radial coordinate frequencies. A resonance between the polar and radial coordinate frequencies is also possible. In the resonance concept, nonlinear perturbations may grow at these radii, ultimately producing X-ray oscillations that represent some combination of the individual resonance frequencies, their sum, or their difference. However, there remain serious uncertainties as to whether such structures could overcome the severe damping forces and emit X-rays with sufficient amplitude and coherence to produce the observed HFQPOs [14].

Models for “diskoseismic” oscillations adopt a more global view of the inner disk as a GR resonance cavity [15, 16]. This paradigm has certain attractions for explaining HFQPOs, but integral harmonics are not predicted for the three types of diskoseismic modes derived for adiabatic perturbations in a thin accretion disk. Clearly, there is also a need to investigate the possibility of resonances within the paradigm of diskoseismology.

As initially noted by Strohmayer [5], the HFQPO measurements may be seen to suggest substantial black hole spin. For the 3 sources with pairs QPOs, optical or IR studies have yielded measurements of the black hole mass. In each case the fastest QPOs exceed the maximum orbital rotation frequency (ν_ϕ) at the innermost stable circular orbit around a Schwarzschild black hole [17] (i.e. dimensionless spin parameter, $a_* = 0$). If the maximum Keplerian frequency is the highest frequency at which a QPO can be seen, then the measurements require prograde spin, e.g. $a_* > 0.15$ for GRO J1655-40. On the other hand, even higher values of the spin parameter are required if the QPOs represent either a resonance in coordinate frequencies [7] ($a_* > 0.25$), or pairs of diskoseismic modes that exhibit commensurate frequencies by chance [18] ($a_* > 0.9$).

Encouragement for linking HFQPOs and GR oscillations can be found in the fact [9] that the HFQPOs in XTE J1550-564 and GRO J1655-40 scale $\sim M^{-1}$. This result is generally consistent with the known mechanisms related to disk oscillations in the strong-field regime of general relativity, as long as the values of the spin parameter (a_*) are similar for these two black holes. These results illustrate both the quantitative value of HFQPO detections as a means of probing the physical properties of black holes, and also the need to continue efforts to independently measure black hole masses via dynamical optical studies. The spin measurements would be of further value towards evaluating the role of black hole rotation in the production of jets [19].

Finally, the investigation of HFQPOs and the the energy spectra for both XTE J1550-564 and GRO J1655-40 show identical patterns of behavior that demand explanation [9]. There is a systematic increase in the strength of the hard X-ray power-law component (i.e. the type with index ~ 2.5) as the observed HFQPO shifts from 3ν to 2ν . We also note that HFQPOs are generally not detected either when the accretion disk dominates the spectrum (i.e. power-law is absent), nor when there is radio emission and the power-law is flatter (index ~ 1.7). These patterns of spectral behavior were used to select the data that yields a new HFQPO detection for GRS 1915+105, as described in the next section.

3. New HFQPOs with Harmonics in GRS 1915+105

GRS 1915+105 is the most extraordinarily variable X-ray binary known [20]. It is also the first member of the “microquasars”, a handful of Galactic X-ray sources that produce relativistic jets [21], as seen in the “superluminal” separation of bipolar knots in sequences of radio images. The system is a confirmed black hole

binary that contains a $\sim 14 M_{\odot}$ black hole [22]. A rich variety of correlations have been found between X-ray, radio, and infrared outbursts [21, 23, 24, 25, 26, 27], contributing substantially to the overall success in linking mass ejections to conditions in the inner accretion disk.

There is an extensive archive of ~ 800 pointed observations of GRS 1915+105 obtained with RXTE during the last six years. About half of these show substantial variability, while the others show roughly steady flux with $\sigma/\mu < 0.18$, evaluated in 1 s bins. Studies of the energy division between the thermal/disk and hard power-law components suggest that most of the steady states are either hard states with persistent radio emission or soft states in which most of the flux originates in the disk [28]. The transient HFQPO at 67 Hz [29] tends to appear in the latter condition, especially when the spectrum is soft and very bright [30]. On the other hand, the steady states of GRS 1915+105 offer limited exposures to conditions when **both** the disk and power-law exhibit high luminosity, which corresponds to the times when harmonic HFQPOs appear in XTE J1550-564 and GRO J1655-40. We are therefore motivated to investigate the variable states of GRS 1915+105, using a scheme to sort the exposures into quadrants of the color-intensity diagram, in order to accumulate significant exposure time when the source is bright and moderately hard.

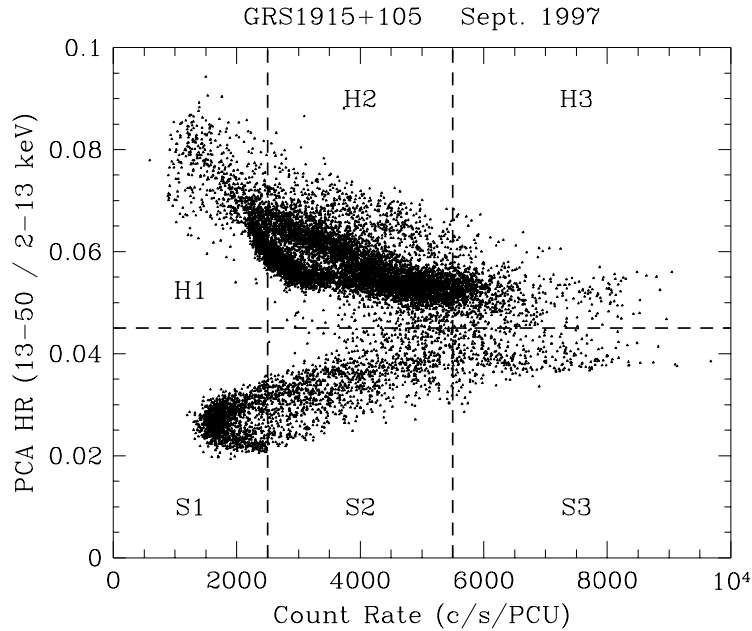


Figure 2. Color-intensity diagram for GRS 1915+105 using RXTE PCA observations on 10 days during 1997 September 5-29. The data from all operating PCUs have been normalized and combined for each 16 s exposure. The dashed lines illustrate the sorting boundaries used to extract times when the source has different levels of the intensity and the relative strength of the power-law component.

For the present analysis, we select the 14 RXTE observations during 1997 September 5-29. These data offer long exposures, some rare bright-hard-steady states, and types of wild variations that include frequent excursions into bright-hard states. The latter cases are highlighted by light curves of the θ classification

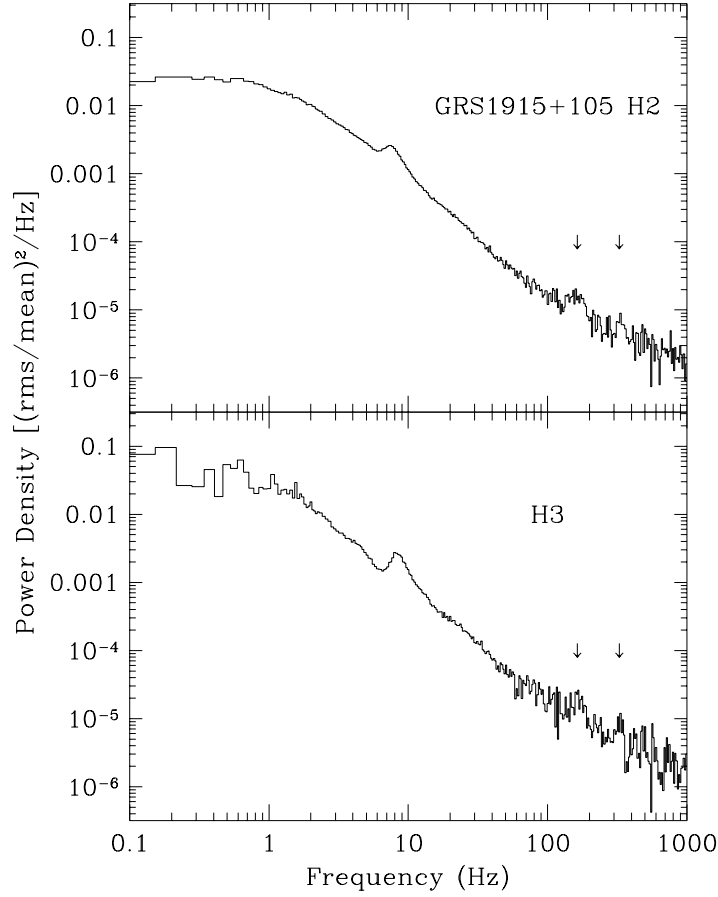


Figure 3. Average power spectrum for groups H2 and H3 (see Fig. 2), selecting only the PCA detections above 13 keV. The arrows indicate weak features at 164 Hz and the locations of the next harmonics (i.e. 328 and 492 Hz).

of Belloni et al. [20]. The background-subtracted PCA spectra are analyzed at a time resolutions of 16 s. The output of all operating PCUs is combined for each time interval, after normalizing each PCU to the characteristics of PCU #2. The PCU normalization is defined using six energy intervals and simply scaling the mean count rate per interval to the results for PCU #2, using the mean spectrum derived for the subset of the observations in which both PCUs were operating. Locations on the color-intensity diagram are computed using a hardness ratio (HR) of normalized source counts at 13–30 keV vs. 2–13 keV. The resulting color-intensity diagram and the data sorting scheme are shown in Fig 2. The hard (“H”) and soft (“S”) regions are separated by the line, $HR = 0.045$, and there are three intensity levels (1,2,3), as shown in the Figure.

The average power density spectra (PDS) are then computed for the data in each of the six regions of the color-intensity diagram. The search for HFQPOs (see methods in [9]) produces detections restricted to regions H2 and H3, using data confined to the energy range of 13–30 keV. These PDS are shown in Fig 3. The H2 PDS shows a peak with a significance of 5.7σ at 163 ± 5 Hz with an rms

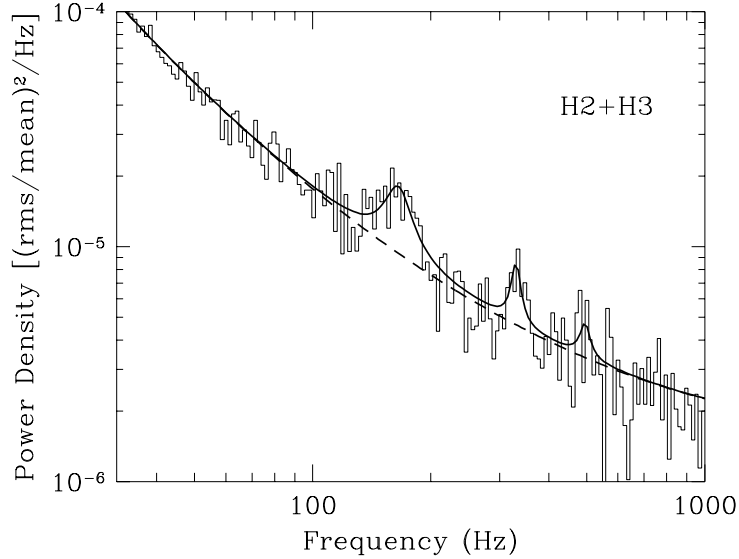


Figure 4. Average power spectrum for groups H2 and H3 (13-30 keV) with the best fit for QPO features and the power continuum. The QPO at 164.9 Hz has a significance of 9σ . The QPO at the first harmonic (329.8 Hz) is detected at 3.7σ , while the hint of a second harmonic (484.8 Hz) is not statistically significant (1.5σ).

amplitude of $1.56 \pm 0.14\%$ of the mean count rate at 13-30 keV. Similarly, the H3 PDS yields a 4.4σ HFQPO at 166 ± 3 Hz with amplitude $1.73 \pm 0.20\%$.

We then combine the H2 and H3 PDS (weighted mean values per bin) and fit the results for an HFQPO with harmonics. The data and best-fit model are shown in Fig 4, and the HFQPO parameters are included in Table 1. With the first harmonic included in the model, the HFQPO at 165 ± 3 Hz has a significance above 9σ . The second peak at 330 Hz has a significance of 3.7σ , while there is a hint (not significant) of the next harmonic at 495 Hz.

In conclusion, the spectral characteristics of HFQPOs in XTE J1550-564 and GRO J1655-40 have provided guidance for finding new HFQPOs at 165 and 330 Hz in GRS 1915+105. The 165 Hz QPO in GRS 1915+105 then appears closely related to the QPO systems with $\nu_0 = 150$ Hz and 92 Hz in GRO J1655-40 and XTE J1550-564, respectively. Given the optical mass estimates for all three black holes, the results suggest faster spin in GRS 1915+105, compared to the other two sources, if the QPOs originate from a common inner disk oscillation related to general relativity. On the other hand, the QPOs at 41 and 67 Hz in GRS 1915+105 may arise from a different physical mechanism.

4. Low Frequency QPOs and Problems in Accretion Physics

The X-ray PDS of many black hole transients display low frequency QPOs (LFQPOs), roughly in the range of 0.05 to 30 Hz. The oscillations can be particularly strong, with peak to trough ratios as high as 1.5 [31]. LFQPOs have been traced out to energy bands as high as 60-124 keV [32]. The measurement properties of

LFQPOs are summarized in Table 2. Some authors pursue separate interpretations for HFQPOs and the more common LFQPOs because they seem to evolve separately and may sometimes coexist [7]. However, others argue that there are unification schemes involving both neutron stars and black holes in which particular mechanisms may operate across a wide range in frequency [33].

Investigations of LFQPO properties versus spectral parameters of the disk and power law components generally show that the LFQPO frequency is most often correlated with the disk flux [34, 35]. However, the rms amplitude generally increases between 2 and 20 keV, and the amplitude spectrum therefore resembles the power-law component rather than the accretion disk [32]. This dualism in correlations encourages LFQPO investigations motivated to deduce the origin of the power-law spectrum. One major complication here is that broad-band spectral studies tend to emphasize the importance of distinguishing two forms of X-ray power law spectra [36]. At highest luminosity (the “very high” state), the spectrum is dominated by a power law with a photon index, $\Gamma \sim 2.5$, which may extend to 500 keV or higher [37]. Alternatively, in the “low/hard” state, the power-law component shows a flatter spectrum ($\Gamma \sim 1.7$) that is cut off above ~ 100 keV, and this state is almost always associated with a steady radio jet [38]. On the other hand, the PDS and QPO properties of these two states may appear rather similar [39, 31].

TABLE 2. Table 2: Properties of Low Frequency QPOs in Black Hole Systems

Property	Value	Comments
Frequency range	0.05 – 30 Hz	most 1–7 Hz
rms amplitude	1 – 20 %	2–30 keV; higher at 6–30 keV
$Q = \nu / \Delta\nu_{FWHM}$	3–30	typical ~ 8.5
Phase Lag	-0.1 – 0.2	2–6 keV vs. 13–30 keV
Harmonics	sometimes 2 and 0.5 ν_0	e.g. XTE J1550 and GRS 1915
In Low-Hard State	often	$\Gamma_{PL} \sim 1.7$ + radio flux
In High-Soft State	no	thermal spectrum, weak power law
In Very High State	yes	defining item; $\Gamma_{PL} \sim 2.5$
Min. Turn-On Timescale	seconds	GRS 1915+105 light curves
Max. Longevity Timescale	months	GRS 1915+105 low-hard state
Freq. Correlation	with Disk Flux	all other params worse
Ampl. Correlation	with Photon Energy	like power-law spectrum, not disk

For the strongest QPOs in GRS 1915+105, efforts were made to track the individual oscillations to determine the origin of the frequency drifts and to measure the average “QPO-folded” oscillation profile [29]. The results show a random walk in QPO phase, with only minor departures from a sinusoidal waveform. The ramifications of this study for QPO models remain uncertain. There are now a large number of proposed LFQPO mechanisms in the literature, and a full review is beyond the scope of this paper. The models include global disk oscillations [40] as well as oscillations in the radial position of complex accretion structures, such as shock fronts [41] or a transition layer between the disk and a hotter Comptonizing region [42]. The construction of complex accretion models is driven not only by the need to account for the power-law spectrum, but also by the relatively slow frequencies of LFQPOs. Given the capacity of LFQPOs for high amplitudes and long-term stability (see Table 2), it would be attractive to associate them with Keplerian frequencies in the disk; however, the relevant disk radii are well

beyond the expected limits of the X-ray emitting region. An alternative model known as the “accretion-ejection instability” invokes spiral waves in a magnetized disk [43], with a transfer of energy out to the radius of corotation with the spiral wave. This model uses magnetic field effects to account for QPOs, the power-law spectrum, and perhaps relativistic outflows as well. Further details are given in other papers of this workshop.

Recent efforts to understand LFQPOs have given attention to the phase lags associated with these oscillations and their harmonics. The analysis technique uses Fourier cross spectra to measure both the phase lags and the coherence parameter (versus frequency) between different X-ray energy bands, e.g. 2-6 vs. 13-30 keV. Unexpectedly, both positive and negative phase lags were found [44, 45, 46, 39], and suggestions were made to classify LFQPOs by phase lag properties [44]. While the expansion of LFQPO subtypes may not be a welcome complication, it has been shown that recognition of the phase lag properties allows us to better understand the relationship between certain types of QPOs and the conditions in the disk [7]. This is illustrated in Fig 5. Furthermore, data selections by LFQPO subtypes provided guidance that helped to establish the harmonic nature of HFQPOs in XTE J1550-564 and the relationship between LFQPOs and HFPQOs in that source [9].

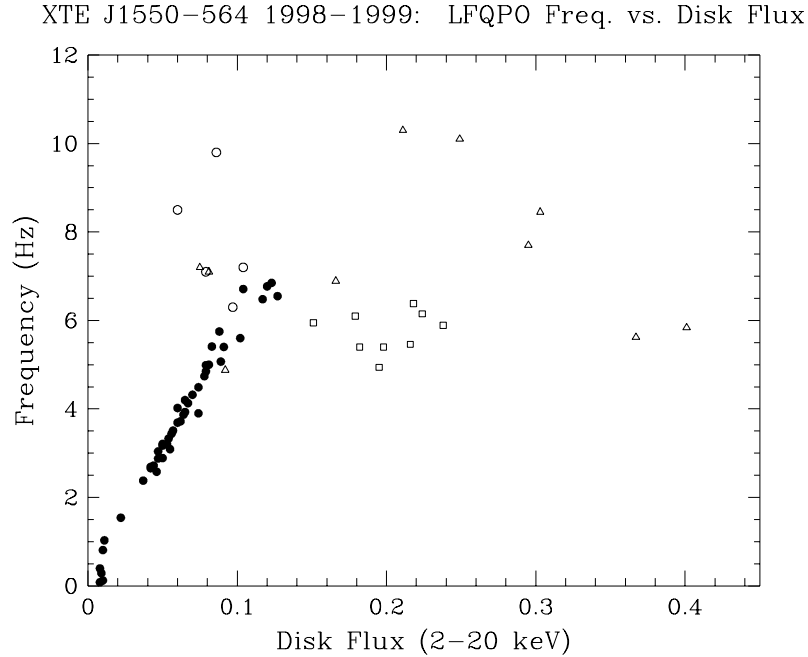


Figure 5. Correlation between LFQPO frequency and the apparent disk flux for XTE J1550-564 during its 1998-1999 outburst. The plotting symbols distinguish the QPO type: Type A (broad QPOs with phase lags in soft X-rays) – open triangles, Type B (narrow QPOs with hard lags) – open squares, Type C (small lags and strong harmonics) – filled circles, and anomalous QPOs – ‘x’. The correlation between these quantities is only demonstrated for the C type LFQPOs.

In closing, it must be noted that the relevance of X-ray timing studies requires discussions of broad power peaks in the PDS [47, 48], which are features wider

than the limit ($Q \sim 2$) used to define QPOs. Broad power peaks are involved in important studies such as the means to distinguish accreting black holes from neutron stars [49]. The evolution of broad power peaks has also been linked to major behavioral changes in a black hole binary, as shown in disappearance of a broad power feature just at the time when Cyg X-1 recently lost its ability to remain in the low-hard state and maintain a steady jet [51].

References

1. Tanaka & Shibazaki, 1996, ARAA, **34**, 607.
2. Meyer-Hofmeister & Meyer, 2001, A&A, **372**, 508.
3. Orosz *et al.*, 2002, ApJ, **568**, 845.
4. van der Klis, 2000, ARAA, **38**, 717.
5. Strohmayer, 2001a, ApJ, **552**, L49.
6. Miller *et al.*, 2001a, ApJ, **563**, 928.
7. Remillard, Sobczak, Munro, & McClintock, 2002a, ApJ, **564**, 962.
8. Strohmayer, 2001b, ApJ, **554**, L169.
9. Remillard, Munro, McClintock, & Orosz, 2002b, ApJ, **580**, in press.
10. Abramowicz & Kluzniak, 2001, A&A, **374**, L19.
11. Stella, Vietri, & Morsink, 1999, ApJ, **524**, L63.
12. Kato, 2001, PASJ, **53**, 1.
13. Merloni, Vietri, Stella, & Bini, 2001, MNRAS, **304**, 155.
14. Markovic & Lamb, 1998, ApJ, **507**, 316.
15. Kato & Fukue, 1980, PASJ, **32**, 377.
16. Wagoner, 1999, Physics Reports, **311**, 259.
17. Shapiro & Teukolsky, 1983, Black Holes, White Dwarfs, and Neutron Stars, (New York: Wiley).
18. Wagoner, Silbergleit, & Ortega-Rodriguez, 2001, ApJ, **559**, L25.
19. Blandford & Znajek, 1977, MNRAS, **179**, 433.
20. Belloni, Klein-Wolt, Mendez, van der Klis, & van Paradijs, 2000, A&A, **355**, 271.
21. Mirabel & Rodriguez, 1999, ARAA, **37**, 409.
22. Greiner, Cuby, & McCaughrean, 2001, Nature, **414**, 522.
23. Eikenberry, Matthews, Morgan, Remillard, & Nelson, 1998, ApJ, **494**, L61.
24. Fender, *et al.*, 1999a, MNRAS, **304**, 865.
25. Fender, *et al.*, 1999b, ApJ, **519**, L165.
26. Dhawan, Mirabel, & Rodriguez, 2000, ApJ, **543**, 373.
27. Corbel *et al.*, 2000, ApJ, **359**, 251.
28. Munro, Morgan, & Remillard, 1999, ApJ, **527**, 321.
29. Morgan, Remillard, & Greiner, 1997, ApJ, **482**, 993.

30. Remillard, Morgan, & Muno, 2000, in Procs. Ninth Marcel Grossman Meeting, July 2000, eds., Gurzadyan, Jantzen, & Ruffini, (Singapore: World Scientific), in press.
31. Sobczak, *et al.* , 2000b, ApJ, **544**, 993.
32. Tomsick & Kaaret, 2001, ApJ, **548**, 401.
33. Psaltis, Belloni, & van der Klis, 1999, ApJ, **520**, 262.
34. Trudolyubov, Churazov, & Gilfanov, 1999, ApL&C, **38**, 233.
35. Sobczak *et al.* , 2000a, ApJ, **531**, 537.
36. Grove, Johnson, Kroeger, McNaron-Brown, Skibo, & Philips, 1998, ApJ, **500**, 899.
37. Tomsick, Kaaret, Kroeger, & Remillard, 1999, ApJ, **512**, 892.
38. Fender, 2001, MNRAS, **322**, 31.
39. Muno, *et al.* , 2001, ApJ, **556**, 515.
40. Titarchuk & Osherovich, 2000, ApJ, **542**, L111.
41. Chakrabarti & Manickam, 2000, ApJ, **531**, L41.
42. Nobili, Turolla, Zampieri, & Belloni, 2000, ApJ, **538**, L137.
43. Tagger & Pellat, 1999, A&A, **349**, 1003.
44. Wijnands, Homan, & van der Klis, 1999, ApJ, **526**, 33.
45. Cui, Zhang, & Chen, 2000, ApJ, **531**, L45.
46. Reig, *et al.* , 2000, ApJ, **541**, 883.
47. Nowak, 2000, MNRAS, **318**, 361.
48. Belloni, Psaltis, & van der Klis, 2002, ApJ, **572**, 392.
49. Sunyaev & Revnivtsev, 2000, A&A, **358**, 617.
50. Revnivtsev, Gilfanov, & Churazov, 2000, A&A, **363**, 1013.
51. Pottschmidt *et al.* , 2002, submitted to A&A (astro-ph/0202258).